Structural divergence of paralogous S components from ECF-type ABC transporters

Ronnie P.-A. Berntsson[1,2], Josy ter Beek[1,2], Maria Majsnerowska[1], Ria H. Duurkens, Pranav Puri, Bert Poolman, and Dirk-Jan Slotboom[3]

Department of Biochemistry, Groningen Biomolecular Sciences and Biotechnology Institute, Netherlands Proteomics Centre and Zernike Institute for Advanced Materials, University of Groningen, Nijenborgh 4, 9747 AG Groningen, The Netherlands

Edited by* Christopher Miller, HHMI, Brandeis University, Waltham, MA, and approved July 23, 2012 (received for review February 24, 2012)

Energy coupling factor (ECF) proteins are ATP-binding cassette transporters involved in the import of micronutrients in prokaryotes. They consist of two nucleotide-binding subunits and the integral membrane subunit EcfT, which together form the ECF module and a second integral membrane subunit that captures the substrate (the S component). Different S components, unrelated in sequence and specific for different ligands, can interact with the same ECF module. Here, we present a high-resolution crystal structure at 2.1 Å of the biotin-specific S component BioY from *Lactococcus lactis*. BioY shares only 16% sequence identity with the thiamin-specific S component ThiT from the same organism, of which we recently solved a crystal structure. Consistent with the lack of sequence similarity, BioY and ThiT display large structural differences (rmsd = 5.1 Å), but the divergence is not equally distributed over the molecules: The S components contain a structurally conserved N-terminal domain that is involved in the interaction with the ECF module and a highly divergent C-terminal domain that binds the substrate. The domain structure explains how the S components with large overall structural differences can interact with the same ECF module while at the same time specifically bind very different substrates with subnanomolar affinity. Solitary BioY (in the absence of the ECF module) is monomeric in detergent solution and binds D-biotin with a high affinity but does not transport the substrate across the membrane.

membrane transport | biotin transport | vitamine uptake

Energy coupling factor (ECF) proteins are an abundant class of ATP-binding cassette (ABC) transporters involved in the import of vitamins and transition metal ions in prokaryotes (1–4). Like all ABC transporters, ECF transporters consist of two cytosolic nucleotide-binding domains (NBDs), which are associated with integral membrane subunits that form the translocation pore. In ECF transporters the two NBDs (EcfA and EcfA', which may be identical or homologous) and a single membrane subunit (EcfT) form a so-called energizing or ECF module. A second integral membrane protein (the S component) binds the substrate and forms a complex with the ECF module to create a functional transporter. This organization is typical for ECF transporters (3–5), because other ABC importers utilize a soluble substrate-binding protein to capture ligands (6, 7). In many ECF transporters multiple S components (specific for different substrates) can interact with the same energizing module (3, 5). Strikingly, S components from a single organism, which interact with the same ECF module, are generally not homologous at the sequence level.

To gain insight in the characteristic modularity of ECF transporters, one needs to compare crystal structures of different S components that interact with the same ECF module (i.e., S components from a single organism). Crystal structures of the S components ThiT from *Lactococcus lactis* (thiamin-specific) and RibU from *Staphylococcus aureus* (riboflavin-specific) (8, 9) have recently been determined. We now present the crystal structure at 2.1 Å of the S component BioY from *Lactococcus lactis*. BioY and ThiT form complexes with the same ECF module (5) and share only 16% sequence identity. We show that BioY from *L. lactis* and the well-studied homologue from *Rhodobacter capsulatus* bind biotin with different kinetics, but neither of the proteins can transport the substrate in the absence of the ECF module.

Results

Selenomethionine (SeMet)-substituted BioY was produced in the expression strain *L. lactis* NZ9000 (10) and purified using the detergent *n*-nonyl-β-D-glucopyranoside, which was also used for the crystallization of RibU and ThiT (8, 9). SeMet-BioY crystals of space group C2 diffracted to 2.1 Å and were used to solve the structure using single-wavelength anomalous diffraction (SAD) phasing (Table 1).

The electron density was of high quality and allowed for modeling of the entire amino acid sequence of BioY, except for the N-terminal tag (MHHHHHHHHA), which was used for metal-affinity purification. After refinement well-defined residual density was observed inside the protein, which could be assigned unambiguously to a D-biotin molecule. In addition, five complete detergent molecules were modeled into densities around the protein. The asymmetric unit contained three copies of BioY that were virtually identical (rmsd < 0.2 Å), with molecule A rotated approximately 90° with respect to B, and molecule C rotated approximately 160° with respect to B (Fig. 1*A*). The relative orientation of the three proteins in the asymmetric unit is incompatible with a membrane environment, and the observed crystallographic trimer is very likely only due to crystal contacts. Indeed, light-scattering experiments (SEC-MALLS) confirmed that BioY is monomeric in detergent solution (Fig. S1).

BioY has six membrane-spanning α-helices (Fig. 1 *A* and *B*). The fold of BioY resembles the folds of RibU and ThiT, but superimposition of all backbone atoms of BioY and either ThiT or RibU revealed large structural differences with rmsds of 5.1 and 4.4 Å, respectively. The structural divergence is not equally distributed over the length of the proteins. BioY, ThiT, and RibU have a structurally very similar N-terminal domain (Helices 1–3) and a highly variable C-terminal domain (Helices 4–6) (Fig. 2). The long membrane-embedded loop between helices 1 and 2 reaches over from the N-terminal to the C-terminal domain and likely has an important functional role (see below).

The structural conservation of the N-terminal halves of S components likely explains their shared use of the ECF module.

Author contributions: R.P.-A.B., J.t.B., M.M., B.P., and D.-J.S. designed research; R.P.-A.B., J.t.B., M.M., R.H.D., P.P., and D.-J.S. performed research; R.P.-A.B., J.t.B., M.M., P.P., B.P., and D.-J.S. analyzed data; and R.P.-A.B., J.t.B., M.M., B.P., and D.-J.S. wrote the paper.

The authors declare no conflict of interest.

*This Direct Submission article had a prearranged editor.

Data deposition: The atomic coordinates and structure factors have been deposited in the Protein Data Bank, www.pdb.org (PDB ID code 4DVE).

[1]R.P.-A.B., J.t.B., and M.M. contributed equally to this work.

[2]Present address: Department of Biochemistry and Biophysics, Arrhenius Laboratories for Natural Sciences, Stockholm University, 10691 Stockholm, Sweden.

[3]To whom correspondence should be addressed. E-mail: d.j.slotboom@rug.nl.

This article contains supporting information online at www.pnas.org/lookup/suppl/doi:10.1073/pnas.1203219109/-/DCSupplemental.

Table 1. Data collection and refinement statistics

Data collection	SeMet-BioY
Space group	C2
Cell dimensions	
a, b, c (Å)	89.8, 57.4, 166.9
α, β, γ (°)	90.0, 91.1, 90.0
Resolution (Å)	48.3–2.1
R_{sym} (%)	6.5 (50.4)
$I/\sigma(I)$	15.3 (2.5)
Completeness (%)	98.4 (90.7)
Redundancy	10.8
Refinement	
Resolution	48.3–2.1
No. unique reflections	47,255
R_{work}/R_{free}	18.5/20.5
No. atoms	
Protein	4,335
Biotin	48
Water	123
B-factors	
Protein	33
Biotin	38
Water	52
R.m.s. deviations	
Bond lengths (Å)	0.015
Bond angles (°)	1.51

Values in parentheses are for highest-resolution shell.

The N-terminal domains of the S components contain a conserved motif (AXXXA, with X mostly hydrophobic amino acids) in helix 1. For ThiT we have shown that the motif is essential for the interaction with the ECF module (8). The alanines of the motif in BioY and ThiT are located at very similar positions on the lipid-exposed face of helix 1.

The variable domain contains the substrate-binding site. BioY was crystallized with a biotin molecule bound to a site near the extracellular face of BioY (Fig. 1*C*). The ligand is mostly occluded, except for the carboxylate tail that has access to the solvent via a narrow tunnel (Fig. 1*D*). The tunnel is too small to allow passage of the biotin molecule. Biotin interacts with helices 4, 5, and 6, and the loop between helix 3 and 4 in the variable domain (Fig. 1*C*). In addition, the loop between helices 1 and 2 from the N-terminal domain directly binds the ligand. The residues involved in biotin binding are conserved among BioY homologues (Fig. S2). The side chains of Asp163 and Lys166, as well as the backbone carbonyl of Pro37 and the backbone NH of Ile39, interact with the imidazole ring. The side chains of Phe159 and Tyr92 stack with the imidazole and thiophene rings of biotin, respectively, and Arg93 interacts with the carboxylate of the pentanoic acid group.

Biotin had not been present during the purification or crystallization procedure, yet the substrate was bound to BioY in the crystals. Apparently, biotin originating from the growth medium remained associated with the protein, indicating slow off rates and high-affinity binding. To produce biotin-free BioY, the expressing cells were cultivated in defined growth medium in the absence of biotin. Biotin binding to the purified *apo*-protein was measured using the intrinsic protein fluorescence titrations. These measurements revealed a protein:biotin binding stoichiometry of 1 : 1 and a dissociation constant K_d of 0.3 nM (Fig. 3*A*).

We reconstituted purified *apo*-BioY into proteoliposomes to determine if BioY could mediate transport of biotin in addition to binding. The reconstituted protein mediated rapid binding of radiolabeled biotin to the proteoliposomes, but the substrate did not accumulate inside the liposomes regardless of whether membrane gradients of protons and sodium ions and a membrane potential of −120 mV were present (Fig. 4*A*). After chasing of the bound radiolabel with an excess of unlabeled biotin, the radioactivity was rapidly released from the proteoliposomes, again indicative of bound rather than transported biotin.

BioY from *L. lactis* is homologous with BioY from *Rhodobacter capsulatus* ($BioY_{RC}$, 35% sequence identity) (2). Transport assays using *Escherichia coli* cells expressing $BioY_{RC}$ have indicated that the protein may transport biotin in the absence of the ECF module (2). To test whether the transport capabilities of $BioY_{RC}$

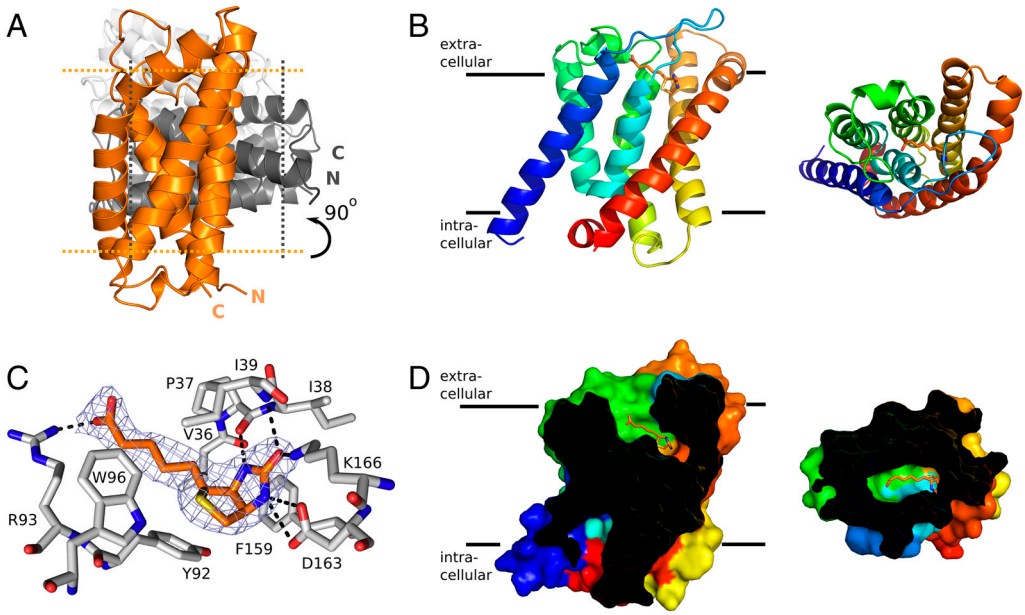

Fig. 1. (*A*) Cartoon showing the relative orientation of the three molecules of BioY in the asymmetric unit of the BioY crystals. The three molecules are colored differently (orange, dark gray, and light gray) and the approximate membrane boundaries are indicated with dotted lines for the orange and dark gray molecules. The trimeric arrangement is incompatible with a membrane-embedded oligomer. (*B*) A monomer of BioY in secondary structure cartoon representation colored from blue (N terminus) to red (C terminus). The bound biotin molecule is shown in stick representation with carbon atoms in orange. The *Left* and *Right* views are from the plain of the membrane and along the membrane normal (from the outside), respectively. (*C*) Binding site of biotin. The biotin molecule is shown in orange and the interacting residues from BioY in gray. Electron density for biotin ($2F_O$-F_C map contoured at 1.5σ) in blue mesh. (*D*) Sliced surface representation of BioY showing the binding cavity, with the bound biotin shown in orange. Coloring and viewpoints as in *B*.

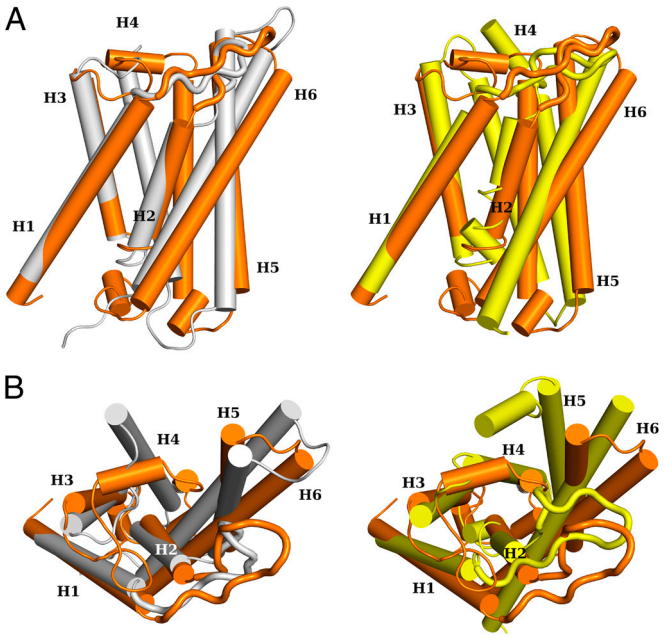

Fig. 2. Superimposed structures of BioY (orange), ThiT (gray), and RibU (yellow) viewed from the plane of the membrane (*A*) and from the outside of the cell (*B*, direction of view perpendicular to the membrane plane). The structures have been superimposed on helices 1 and 3 in order to highlight the structural similarities of helices 1–3 and the differences of helices 4–6. Loops 1 are indicated in thick lines. Helices 1–6 are marked with H1–H6.

are indeed different than those of BioY from *L. lactis*, we also purified and membrane-reconstituted $BioY_{RC}$. Biotin bound rapidly to the proteoliposomes containing *apo*-$BioY_{RC}$, just like it did to BioY from *L. lactis*, and again no accumulation was observed, neither in the presence nor in the absence of membrane gradients for protons and sodium ions and a membrane potential (Fig. 4*B*). However, the kinetics of the subsequent chase of radiolabeled biotin from the proteoliposomes with an excess of unlabeled biotin was much slower than in the case of the lactococcal protein. The fast association of radiolabeled biotin with the proteoliposomes and the slow chase are indicative of biotin binding with fast on rates and slow off rates compared to *L. lactis* BioY. To test whether substrate release indeed was slow, we repeated the binding experiment using proteoliposomes in which $BioY_{RC}$ was saturated with unlabeled biotin at the start of the experiment instead of using *apo*-$BioY_{RC}$ (Fig. S3). In this case, the apparent binding rates of radiolabeled biotin were slow and similar in magnitude to the release rates of the chase experiment, indicating that indeed the off rates were limiting in the experiment and showing that $BioY_{RC}$ alone is a binding protein rather than a transporter. To further confirm that $BioY_{RC}$ does not mediate transport of biotin we performed a counterflow experiment (Fig. 4*B*). If exchange of biotin between the luminal pool of unlabeled biotin (15 μM) and the external radiolabeled pool (150 nM) were to occur, an apparent accumulation of the radiolabel should become apparent. However, the same amount of radiolabel associated with the loaded proteoliposomes as in the case where unloaded liposomes were used, again showing that binding but not transport took place.

The low k_{off} rate of biotin from $BioY_{RC}$ is indicative of very high affinity binding. Indeed, fluorescence titrations showed that biotin binds with high affinity to $BioY_{RC}$ (Fig. 3*B*), but it was impossible to accurately determine the K_d, because the change in fluorescence upon biotin binding was small. Therefore, high protein concentrations were needed in the assay to obtain good signal-to-noise ratios, which is incompatible with accurate determination of low K_d values.

Discussion

The ECF module from *L. lactis* can interact with eight different S components, six of which share less than 20% sequence identity with any of the other S components in the organism (5). For two of the S components from *L. lactis*, BioY, and ThiT, we now have determined crystal structures at high resolution. There is large structural variation between BioY and ThiT, with the two proteins displaying an rmsd of 5.1 Å. The structural differences are in line with the lack of sequence conservation (16% identity between BioY and ThiT). Most variation is in the C-terminal domain (helix 4–6), which is involved in substrate binding. The substrates thiamin and biotin are chemically very different explaining the large structural variation in the binding domains. Similarly, the C-terminal domain of the riboflavin-binding S component RibU from *S. aureus*, for which a crystal structure of moderate resolution is available, is structurally divergent. The N-terminal domains (consisting of helices 1–3) are more similar in all structures and—at a the same position in helix 1—contain the AXXXA motif that was found to be essential for thiamin transport by the ECF module-ThiT complex (8). Although BioY, ThiT from *L. lactis* and RibU from *S. aureus* are structurally very different, there are also similarities. In all three proteins, not only residues from the nonconserved C-terminal domain interact with the substrate but also residues from the loop between helices 1 and 2 in the N-terminal domain (residues 36–39 in BioY). Loop 1–2 forms a direct link between the substrate-binding site and the N-terminal domain that interacts with the ECF module. The loop therefore may mediate coupling between conformational changes in the ECF module induced by ATP-binding/hydrolysis and substrate binding/release in the S component (Fig. 2). In response to

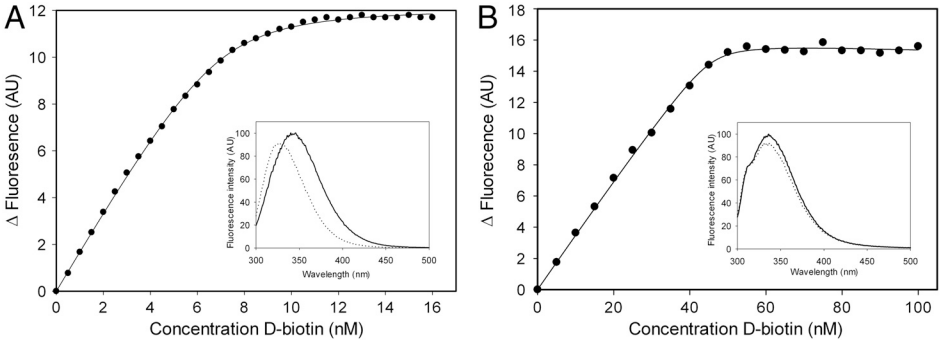

Fig. 3. Biotin binding to BioY. (*A*) Titration of 10 nM BioY with D-biotin. The intrinsic protein fluorescence was measured (excitation wavelength 280 nm, emission wavelength 360 nm). *Inset*: fluorescence spectrum of 300 nM BioY in the absence of biotin (solid line) and in the presence of a saturating amount of biotin (1 mM, dotted line). (*B*) Biotin binding to $BioY_{RC}$. Titration of 50 nM BioY from *Rhodobacter capsulatus* with D-biotin. The intrinsic protein fluorescence was measured (excitation wavelength 280 nm, emission wavelength 349 nm). *Inset*: fluorescence spectrum of BioY in the absence of biotin (solid line) and in the presence of a saturating amount of biotin (100 nM, dotted line).

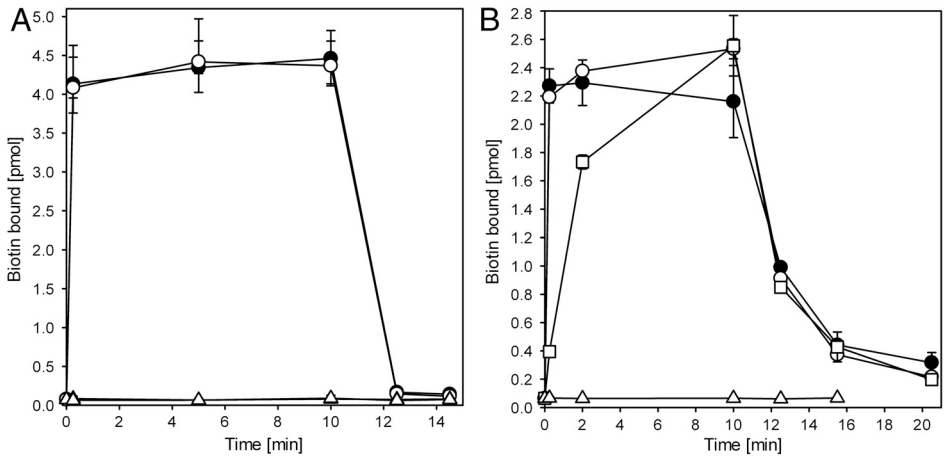

Fig. 4. Biotin binding to liposomes containing purified and reconstituted BioY from *L. lactis* (*A*) and $BioY_{RC}$ from *R. capsulatus* (*B*), respectively. Biotin binding was measured in the presence (black circles) or absence (white circles) of membrane gradients of proton gradient, sodium ions, and a membrane potential (−120 mV). Black and white triangles represent the same experiment using liposomes without BioY. After 10.5 min an excess (1 mM) of unlabeled biotin was added. 160 μg lipids (approximately 1.6 μg of BioY) was used per time point. Squares in *B*: counterflow experiment. Proteoliposomes were loaded with 15 μM unlabeled biotin before 100-fold dilution into buffer containing 20 nM labeled biotin to start the experiment. All experiments were performed in duplicate or triplicate, and the error bars represent the spread in the data. The amounts of biotin bound to the liposomes in (*B*) is lower than in (*A*) because the $BioY_{RC}$ is less stable in detergent solution (prone to aggregation) causing lower reconstitution efficiencies of functional protein.

ATP-binding/hydrolysis in the ATPase domains, the loop may rearrange and thereby perturb the substrate-binding site while at the same time opening up the pathway for substrate translocation. Because loop 1–2 is located on the external face of the S components, whereas the nucleotide-binding domains are cytoplasmic, the ATP-dependent conformational changes will have to be communicated/transduced via a transmembrane protein (e.g. the EcfT subunit).

BioY from *L. lactis* and BioY from *Rhodobacter capsulatus* ($BioY_{RC}$) share 35% sequence identity. The latter protein is the archetypical member of the S component superfamily (2). Based on the characterization of $BioY_{RC}$ expressed in *E. coli* cells it has been suggested that the BioY-family of S components may be different from other S components both in terms of oligomeric structure and in terms of transport mechanism. Nonetheless, our biochemical and structural characterization of BioY suggest a unifying structure and mechanism.

First, the stable structural unit of BioY in detergent solution is a monomer. Analysis of the crystal packing showed that adjacent BioY molecules in the crystals do not represent physiological oligomers, because their relative orientations are incompatible with embedding in a membrane environment. In addition, static light scattering experiments (SEC-MALLS) confirmed that BioY is monomeric, just like other S components such as ThiT (11) and RibU (9). Similarly, we found that $BioY_{RC}$ from *Rhodobacter capsulatus* is monomeric in detergent solution (12). Therefore, from a structural point of view the BioY-family is not different from other S components. In contrast, in vivo fluorescence lifetime measurements have indicated that $BioY_{Rc}$ forms oligomers when heterologously overproduced in *E. coli*. We cannot exclude that the oligomeric state of S components is different in membranes, but none of the available structures (BioY, ThiT and RibU) show possibilities for extensive interfaces, which would be required for stable oligomer formation. Therefore the structure in membranes must be different, were oligomerization to occur.

Second, D-biotin binds to BioY with a high affinity (K_d of 0.3 nM). The affinity measured in vitro compares well to the K_d of 0.15 nM that was found in the 1970s for biotin binding to whole cells of *L. casei* (13), which was likely mediated by a BioY orthologue. Fluorescence titrations showed the presence of a single binding site per BioY molecule, which is consistent with the crystal structure. Subnanomolar K_d values and 1 : 1 binding stoichiometry are conserved features of S components (11, 13–16), and these properties are also conserved in $BioY_{RC}$ from *R. capsulatus* (Fig. 3).

Third, in the absence of the ECF module, $BioY_{RC}$ from *R. capsulatus* was reported to be a low-affinity, high-capacity transporter when overexpressed heterologously in *E. coli* cells (2). Such transport kinetics combined with the high affinity binding that we find for BioY and $BioY_{RC}$ would require input of free energy. However, regardless of the presence of membrane gradients for protons and sodium ions, and a membrane potential, we could not detect transport of biotin by BioY from *L. lactis* or $BioY_{RC}$ reconstituted in proteoliposomes. The reconstituted proteins supported binding of radiolabeled biotin only. Therefore, we conclude that, in the absence of the ECF module, BioY from *L. lactis* and $BioY_{RC}$ act as a high-affinity substrate-binding protein and that they cannot transport biotin on their own.

How then can we explain the apparent biotin transport reported for $BioY_{RC}$ expressed in *E. coli* cells? Our data show that the release of bound biotin from solitary $BioY_{RC}$ is very slow (low off rate, Fig. 4*B* and Fig. S3). In the paper where solitary $BioY_{RC}$ was reported to transport biotin (2) the protein most likely was biotin-saturated rather than *apo* at the onset of the experiment. We hypothesize that these experiments showed slow exchange of the bound, unlabeled biotin for radiolabeled substrate rather than transport.

The lack of transport activity by solitary BioY is consistent with the absence of an obvious translocation path through BioY. Most of the conserved residues in BioY are involved in either ligand binding (near the extracellular face of the protein) or tight packing of the helices (many glycines; Fig. S2) or interaction with the ECF module (AXXXA motif). In contrast, a speculative pathway for the transport of riboflavin through solitary RibU was proposed based on the presence of conserved residues in the RibU family (9). We reevaluated the residue conservation in RibU and found that the proposed pathway-lining residues are not conserved when a larger set of sequences was used [Erkens et al. (8) and Fig. S2]. Therefore, we believe that there is no evidence for a translocation path through the protein, which is consistent with the experimental observation that RibU alone does not support uptake of riboflavin in cells (9). Similarly, ThiT does not support transport of thiamin, and the structure does not show a translocation pathway. Also the S components for folate and pantothenate cannot transport their substrates without the ECF module (3, 17). We conclude that S components in the absence of

additional components are binding proteins rather than transporters (8). Together with the ECF module, they form a substrate translocation path across the membrane.

Materials and Methods

Protein Expression. Selenomethionine-substituted BioY containing a N-terminal decahistidine tag was expressed in *Lactococcus lactis* strain NZ9000 (18), as previously described (19). Briefly, the cells were grown semi-anaerobically in chemically defined medium (CDM) to an OD_{600} of 1.5. At this point, the cells were spun down and resuspended in CDM with selenomethionine instead of methionine. After 20 min, *bioY* expression was induced by the addition of 0.1% (v/v) of culture supernatant from the nisin A-producing strain NZ9700 (18). The cells were grown to an OD_{600} of 4 and then harvested by centrifugation and subsequently resuspended in buffer A (50 mM Na-Hepes pH 7.5, 300 mM NaCl and 10% (v/v) glycerol).

Cell lysis was performed by passing the cells twice trough a cell disruptor (Constant Systems Ltd.) at a pressure of 39 kPsi, 4 °C. Prior to the disruption, $MgSO_4$ (5 mM) and DNase (100 μg/mL) were added. Unbroken cells were removed by centrifugation at 6,000 × *g*, 15 min, 4 °C. Membrane vesicles were collected by a subsequent centrifugation at 267,000 × *g* for 80 min at 4 °C, and resuspended and homogenized in buffer A to a protein concentration of 40 mg/mL, flash frozen in liquid nitrogen and stored at −80 °C.

Protein Purification. Membrane vesicles (100 mg total protein) were thawed and diluted in buffer A to approximately 5 mg/mL total protein. Solubilization was done by the addition of 1% (w/v) of dodecyl-β-D-maltoside and incubation at 4 °C for 1 h (the mixture was mixed by gentle rotation). Unsolubilized material was spun down at 267,000 × *g* and 4 °C for 20 min. 0.5 mL Ni-Sepharose plus 15 mM imidazole pH 7.8 were added to the supernatant, and the mixture was incubated at 4 °C for 1 h (under gentle rotation). The suspension was poured into a 10-mL disposable column (Bio-Rad), and the flow-through was discarded. The column was washed with 20 column volumes of buffer B [50 mM Na-Hepes pH 7.5, 300 mM NaCl, 50 mM imidazole pH 7.8 plus 0.35% (w/v) *n*-nonyl-β-D-glucopyranoside (NG, Anatrace)]. The protein was eluted from the column in 2 fractions (0.35 and 0.75 mL, respectively) with buffer B supplemented with 500 mM imidazole pH 7.8. The second elution fraction was loaded onto a Superdex 200 10/300 GL gel filtration column (GE Healthcare), equilibrated with buffer C (20 mM Na-Hepes pH 7.5, 150 mM NaCl plus 0.35% (w/v) NG). Peak fractions were concentrated to 7 mg/mL, using a Vivaspin 30 kDa molecular weight cutoff concentrator (VVR International) and immediately used for crystallization trials or other biochemical assays.

For biochemical characterization of BioY, the protein was purified from cells grown in CDM without biotin (for the isolation of substrate-free protein). The purification protocol was slightly modified: Solubilization was done in a buffer containing 50 mM potassium-phosphate, 300 mM NaCl, 10% glycerol plus 1% maltose-neopentyl glycol 3 (MNG-3) (20), pH 7.5. The nickel-sepharose column was washed with 20 column volumes of 50 mM potassium phosphate, pH 7.5, 300 mM NaCl, 10% glycerol, 50 mM imidazol plus 0.03% MNG-3, and eluted with the same buffer supplemented with 500 mM imidazol. Size-exclusion chromatography was done in 50 mM potassium phosphate, pH 7.5, 150 mM NaCl plus 0.03% MNG-3.

Crystallization. Initial crystal hits of BioY were found in several conditions, all containing high concentrations of PEG and pH values between 7 and 9. Optimization of the conditions yielded diffraction-quality crystals with a size of ca 100 × 50 × 50 μm. The best crystals were grown at 5 °C with the reservoir solution containing 0.1 M Tris pH 8.0, 0.05–0.2 mM $CaCl_2$ plus 45–50% PEG400. Due to the high PEG400 concentration, no further cryo-protectant was needed, and the crystals were directly fished from the drop and flash frozen in liquid nitrogen.

Structure Determination. Diffraction data was collected at the PX1 beam-line at the Swiss Light Source. Single-wavelength Anomalous Dispersion (SAD) data on SeMet-BioY was collected to 2.1 Å, at 100 K with a wavelength of 12.657 keV. Data processing and reduction were carried out, using XDS (21) and programs from the CCP4 suite (22). Relevant statistics can be found in Table 1. Initial phase information was found using autoSharp (23) and an initial model containing 95% of the residues could be built using ARP/warp (24). Fifteen selenium sites were found within the asymmetric unit, corresponding to all five of the possible sites per BioY molecule. A few cycles of refinement using Refmac5 (25), and noncrystallographic symmetry with loose restraints, interspersed with manual model building in Coot (26), were necessary to finish the model. Water molecules were automatically placed in F_O-F_C Fourier difference maps at 3σ cutoff levels and validated to ensure correct positioning, using Coot. The final protein model contains residues 1–188 for all three molecules in the asymmetric unit. Electron density that could correspond to acyl chains (without visible density for headgroups) was not modeled. R_{work} and R_{free} of the final model after refinement were 18.6% and 20.6%, respectively. All structure figures were prepared using PyMOL.

Fluorescence Titration. Tryptophan fluorescence was measured in a stirred quartz cuvette on a SPEX Fluorolog 322 fluorescence spectrophotometer (Jobin Yvon) at 25 °C. Purified biotin-free BioY was diluted in size-exclusion chromatography buffer to the indicated concentration (final volume 1,000 μL). D-biotin was added in 0.5 μL steps. The excitation and emission wavelengths were 280 nm and 360 nm, respectively. The data was analyzed as described in Erkens et al. (11). Because of the high-affinity binding by BioY, the protein was diluted to approximately 10 nM for titrations with biotin. For BioY from *R. capsulatus*, the fluorescence measurements were done in the same way, except that the emission wavelength was 349 nm and that the protein concentration was approximately 50 nM.

Light Scattering. The oligomeric state of BioY was determined via size-exclusion chromatography coupled to multi-angle laser light scattering (SEC-MALLS) as described before (5, 11). We used BioY isolated from cells grown on rich medium (with biotin) that was purified in the same way as the biotin-free protein.

Uptakes by Proteoliposomes Containing BioY. Substrate-free BioY (in a buffer of 50 mM potassium phosphate, pH 7.5, 150 mM NaCl plus 0.03% MNG-3) was reconstituted into proteoliposomes at a protein:lipid ratio of 1:100 (w/w), essentially as described in ref. (5). Proteoliposomes were subjected to three cycles of freeze-thawing using liquid nitrogen, extruded through a 400 nm pore size polycarbonate filter (Avestin), and centrifuged (267,000 rcf, 4 °C, 40 min, Beckman TLA 100.4 rotor) in 50 mM potassium phosphate, pH 7.5. For transport assays, 2 μL of proteoliposomes (80 μg/μL lipid concentration) were diluted into 200 μL of buffers containing 20 nM [^{3}H]biotin and 150 nM unlabeled biotin. Different buffer compositions were used depending on whether membrane gradients were required: (*i*) 57 mM sodium phosphate pH 6.5 containing 1 μM valinomycin (diluted from a 3 mM stock in ethanol) to obtain gradients for protons and sodium ions in combination with membrane potential; (*ii*) 50 mM potassium phosphate pH 7.5 (no gradients). Buffers were pre-warmed to 25 °C and the suspension was briefly vortexed after addition of proteoliposomes. At the indicated times 2 mL of ice-cold 50 mM potassium phosphate pH 7.5 was added followed by rapid filtration over 0.45 μm pore-size cellulose nitrate filter (Whatman Maidstone UK). The filters were washed once with 2 mL ice-cold 50 mM potassium phosphate pH 7.5. Background signal was determined by using liposomes without BioY. Radioactivity trapped on the filters was measured by addition of 2 mL of emulsifier plus scintillation liquid and subsequent counting in a Perkin Elmer 1600CA scintillation counter.

ACKNOWLEDGMENTS. This work was supported by grants from the Netherlands Organisation for Scientific Research (NWO: top-talent grant to J.t.B., Vidi and Vici grant to D.-J.S., top-subsidy grant 700.56.302 to B.P.) and the European Union (European Research Council starting grant to D.-J.S. and EDICT program). We acknowledge Pil Seok Chae for the gift of MNG-3.

1. Rodionov DA, Hebbeln P, Gelfand MS, Eitinger T (2006) Comparative and functional genomic analysis of prokaryotic nickel and cobalt uptake transporters: Evidence for a novel group of ATP-binding cassette transporters. *J Bacteriol* 188:317–327.
2. Hebbeln P, Rodionov DA, Alfandega A, Eitinger T (2007) Biotin uptake in prokaryotes by solute transporters with an optional ATP-binding cassette-containing module. *Proc Natl Acad Sci USA* 104:2909–2914.
3. Rodionov DA, et al. (2009) A novel class of modular transporters for vitamins in prokaryotes. *J Bacteriol* 191:42–51.
4. Erkens GB, Majsnerowska M, Beek ter J, Slotboom D-J (2012) Energy coupling factor-type ABC transporters for vitamin uptake in prokaryotes. *Biochemistry* 51:4390–4396.
5. Beek ter J, Duurkens R, Erkens G, Slobtoom DJ (2010) Quaternary structure and functional unit of Energy Coupling Factor (ECF)-type transporters. *J Biol Chem* 286:5471–5475.
6. Higgins CF (1992) ABC transporters: From microorganisms to man. *Annu Rev Cell Biol* 8:67–113.
7. Berntsson RP-A, Smits SHJ, Schmitt L, Slotboom D-J, Poolman B (2010) A structural classification of substrate-binding proteins. *FEBS Lett* 584:2606–2617.
8. Erkens GB, et al. (2011) The structural basis of modularity in ECF-type ABC transporters. *Nat Struct Mol Biol* 18:755–760.
9. Zhang P, Wang J, Shi Y (2010) Structure and mechanism of the S component of a bacterial ECF transporter. *Nature* 468:717–720.

10. Kunji ERS, Slotboom D-J, Poolman B (2003) *Lactococcus lactis* as host for overproduction of functional membrane proteins. *Biochim Biophys Acta* 1610:97–108.
11. Erkens GB, Slotboom D-J (2010) Biochemical characterization of ThiT from *Lactococcus lactis*: A thiamin transporter with picomolar substrate binding affinity. *Biochemistry* 49:3203–3212.
12. Finkenwirth F, et al. (2010) Subunit composition of an energy-coupling-factor-type biotin transporter analysed in living bacteria. *Biochem J* 431:373–380.
13. Henderson GB, Kojima JM, Kumar HP (1985) Differential interaction of cations with the thiamine and biotin transport proteins of *Lactobacillus casei*. *Biochim Biophys Acta* 813:201–206.
14. Duurkens RH, Tol MB, Geertsma ER, Permentier HP, Slotboom D-J (2007) Flavin binding to the high affinity riboflavin transporter RibU. *J Biol Chem* 282:10380–10386.
15. Eudes A, et al. (2008) Identification of genes encoding the folate- and thiamine-binding membrane proteins in Firmicutes. *J Bacteriol* 190:7591–7594.
16. Henderson GB, Zevely EM (1978) Binding and transport of thiamine by *Lactobacillus casei*. *J Bacteriol* 133:1190–1196.
17. Neubauer O, et al. (2009) Two essential arginine residues in the T components of energy-coupling factor transporters. *J Bacteriol* 191:6482–6488.
18. de Ruyter PG, Kuipers OP, de Vos WM (1996) Controlled gene expression systems for *Lactococcus lactis* with the food-grade inducer nisin. *Appl Environ Microbiol* 62:3662–3667.
19. Berntsson RP-A, et al. (2009) Selenomethionine incorporation in proteins expressed in *Lactococcus lactis*. *Protein Sci* 18:1121–1127.
20. Chae PS, et al. (2010) Maltose-neopentyl glycol (MNG) amphiphiles for solubilization, stabilization and crystallization of membrane proteins. *Nat Methods* 7:1003–U90.
21. Kabsch W (1993) Automatic processing of rotation diffraction data from crystals of initially unknown symmetry and cell constants. *J Appl Crystallogr* 26:795–800.
22. Collaborative Computational Project, Number 4 (1994) The CCP4 suite: Programs for protein crystallography. *Acta Crystallogr D Biol Crystallogr* 50:760–763.
23. Vonrhein C, Blanc E, Roversi P, Bricogne G (2007) Automated structure solution with autoSHARP. *Methods Mol Biol* 364:215–230.
24. Langer G, Cohen SX, Lamzin VS, Perrakis A (2008) Automated macromolecular model building for X-ray crystallography using ARP/wARP version 7. *Nat Protoc* 3:1171–1179.
25. Murshudov GN, Vagin AA, Dodson E (1997) Refinement of macromolecular structures by the maximum-likelihood method. *Acta Crystallogr D Biol Crystallogr* 53:240–255.
26. Emsley P, Cowtan K (2004) Coot: Model-building tools for molecular graphics. *Acta Crystallogr D Biol Crystallogr* 60:2126–2132.